Optica Applicata, Vol. XLI, No. 2, 2011

Electrical and photoelectric characterization of the MOS structures on 3C–SiC substrate

KRZYSZTOF PISKORSKI[1*], HENRYK M. PRZEWŁOCKI[1], ROMAIN ESTEVE[2], MIETEK BAKOWSKI[2]

[1]Institute of Electron Technology, Department of Characterization of Nanoelectronic Structures, al. Lotników 32/46, 02-668 Warsaw, Poland

[2]Acreo AB, Electrum 236, SE-164 40 Kista, Sweden

[*]Corresponding author: kpisk@ite.waw.pl

In this work results are presented of the electrical and photoelectric measurements of MOS capacitors, consisting of an Al gate of thickness 25 nm, SiO_2 insulator of thickness 60 nm, and *n*-doped 3C–SiC. Many different measurement techniques are employed in order to completely define all parameters of the band diagram of the MOS structure, which is the main goal of these investigations.

Keywords: silicon carbide (SiC), MOS structure, band diagram.

1. Introduction

Silicon carbide (SiC) is an attractive material for electronic applications due to good electrical and thermal properties. The most important properties for further development of modern electronic devices are the wide bandgap (from 2.36 eV (3C type) to 3.23 eV (4H type)) [1], high breakdown field and good thermal conductivity. Due to its lower bandgap, the 3C–SiC has lower breakdown field than the 4H–SiC. However, the inversion channel mobility observed in 3C–SiC is more than one order of magnitude higher compared to 4H–SiC. This is because the near interface traps (NIT) that limit the channel mobility in the 4H–SiC MOSFETs are positioned in the conduction band and not in the bandgap in 3C–SiC [2, 3]. The 3C–SiC devices are furthermore characterized by lower specific junction capacitance. They are also expected to be more cost effective due to the availability of large substrate sizes since the 3C–SiC material is grown on state of the art sized silicon wafers [4]. All these advantages make 3C–SiC material suitable for medium power (600 V and 1200 V) and high frequency devices.

Understanding of the physical properties of MOS structures on 3C–SiC is of importance for device development and optimization. The electrical properties of

a range of MOS capacitors built on 3C–SiC epilayers were investigated. The capacitors under investigation differed in the way the dielectric layer was formed and in the gate material. The capacitors consisted of two groups: while the first group was based on *ca.* 60 nm of thermal SiO_2 grown by thermal oxidation in wet oxygen (H_2O:O_2) at 1150 °C for 70 min, the second one has been formed using an advanced oxidation process combining thermal and deposited oxide. This advanced oxidation process allows to deposit *ca*. 55 nm of silicon dioxide using plasma enhanced chemical vapor deposition (PECVD) and to post-oxidize it in wet oxygen (H_2O:O_2) at 950 °C for 3 h. The post-oxidation step performs firstly a densification of the deposited oxide and secondly a thermal oxidation of a 3–5 nm thick layer of SiC. In each of these groups, four different materials were deposited on top of the SiO_2 layer to form the gate: polysilicon, aluminum, gold and nickel.

This report is limited to a description of the band diagram determination for just one subgroup of the investigated samples, namely for the MOS capacitors with an aluminum gate and the SiO_2 layer deposited by PECVD on 3C–SiC substrates.

2. Experiment

MOS capacitors were fabricated on free standing 3" *n*-type 3C–SiC (001) wafers with about 10 μm thick *n*-type epitaxial layer nitrogen doped in the mid 10^{15} cm^{-3} on top. A SiO_2 layer of thickness $t_{OX} \approx 55$ nm was deposited by PECVD after which the wafers were subjected to the so-called post-oxidation anneal in wet oxygen for 3 h at 950 °C. Circular aluminum metal contacts 0.7 mm in diameter and with thickness $t_{Al} = 25$ nm were formed by ion beam sputtering and lift-off.

Electrical and photoelectric measurements were carried out using the multifunctional system for photoelectric measurements (MSPM), which has been described elsewhere [5]. The oxide thickness t_{OX} was determined from capacitance–voltage $C = f(V_G)$ measurements. The results were compared with results obtained by spectroscopic ellipsometry. No significant difference was observed between the results from each of these methods. The substrate doping density N_D was calculated from $1/C^2$ vs. V_G plots, obtained from $C = f(V_G)$ measurements.

Experimental photocurrent I_F vs. wavelength λ characteristics were recorded at different gate voltages V_G in order to determine barrier heights on both sides of the dielectric. Due to optical interference in the dielectric layer and the strong dependence on wavelength λ of light absorption in the substrate, the quantum yield Y vs. photon energy $h\nu$ characteristics were calculated taking into account the optical properties of the MOS structure. These properties were calculated using procedures which were similar to the ones described in [6].

3. Measurement procedures

The energy band diagram of a MOS structure, as a representation of different potentials existing in the structure, is usually determined from many measurement techniques.

These techniques can be divided into three different groups: electrical, photoelectric and optical. These permit determination of all necessary parameters which are important in modern semiconductor devices (*e.g.*, flat-band voltage in semiconductor V_{FB}, the effective contact potential difference ϕ_{MS}). Some of these parameters can be directly obtained from an appropriate measurement technique (*e.g.*, flat-band voltage in the dielectric V_{G0} from $I_F = f(V_G)$ characteristics). However, determination of other parameters requires calculations based on measurement results (*e.g.*, substrate doping density N_D, which is calculated from the slope of a $1/C^2 = f(V_G)$ plot). A short description of every method used in this work follows.

3.1. Electrical measurements

The basic test structure for determination of MOS system parameters is the MOS capacitor. Usually, a $C = f(V_G)$ characteristic of this capacitor is measured, and the flat-band voltage V_{FB} is probably the most important parameter deduced from this characteristic. V_{FB} is the gate voltage required to achieve the flat-band condition at the semiconductor–dielectric interface. The value of V_{FB} is important since this parameter is directly related to the threshold voltage V_T of MOS transistors.

The experimental $C = f(V_G)$ characteristics (dark and illuminated) measured at signal frequency of $f = 1$ MHz and a calculated theoretical characteristic for an ideal MOS structure are shown in Fig. 1. The illuminated $C^* = f(V_G)$ characteristic is used to determine the surface potential of the semiconductor ϕ_{S0}, as described in Section 3.3. Measurements were made on Al–SiO_2–SiC(3C) structure with a SiO_2 thickness $t_{OX} \approx 60$ nm.

An important feature of the dark $C = f(V_G)$ characteristic presented in Fig. 1 is that it is shifted toward a more negative gate voltage in comparison to the theoretical characteristic of the ideal MOS structure. This shows that a large positive effective oxide charge Q_{eff} resides in the structures on 3C–SiC substrate.

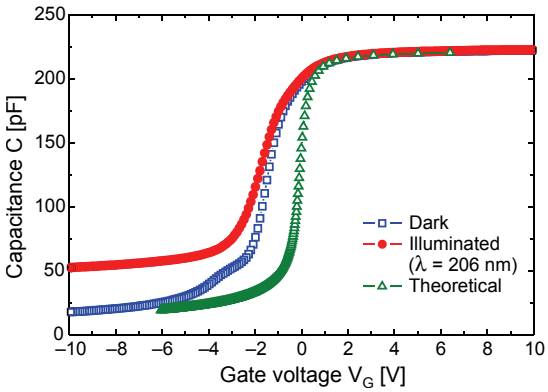

Fig. 1. Experimental $C = f(V_G)$ characteristics (dark and illuminated) measured at signal frequency of $f = 1$ MHz on the Al–SiO_2–SiC(3C) structure. Also a calculated theoretical characteristic is shown for comparison.

The V_{FB} value can be obtained in many ways [7–10]. However the most common method to determine V_{FB}, and which is used in this work, is the method based on calculation of the flat-band capacitance C_{FB} [7]:

$$C_{FB} = \frac{C_{OX} C_{sFB}}{C_{OX} + C_{sFB}} \tag{1}$$

where: C_{OX} – capacitance in the accumulation state [F/cm^2], C_{sFB} – semiconductor surface capacitance [F/cm^2] expressed by:

$$C_{sFB} = \frac{\varepsilon_S \varepsilon_0}{L_D} \tag{2}$$

where: ε_S – electrical permittivity of the semiconductor, ε_0 – electrical permittivity of vacuum [F/cm], L_D – Debye's length [cm] given as:

$$L_D = \sqrt{\frac{kT\varepsilon_S \varepsilon_0}{q^2 N_D}} \tag{3}$$

where: k – Boltzmann's constant [J/K], T – temperature [K], q – electron charge [C].

After calculating the C_{FB} value, the flat-band voltage V_{FB} is obtained from the measured $C = f(V_G)$ characteristic. In order to calculate the C_{FB} value, the substrate doping density N_D has to be known. N_D can be determined from $C = f(V_G)$ measurements. The simplest way to determine N_D is to use the following formula, where the slope (in [F^{-1}C^{-1}]) of the linear part of a $1/C^2 = f(V_G)$ plot is utilized [7]:

$$N_D = \frac{2}{q\varepsilon_S \varepsilon_0} \frac{1}{|\text{slope}| A^2} \tag{4}$$

where A – gate area [cm^2].

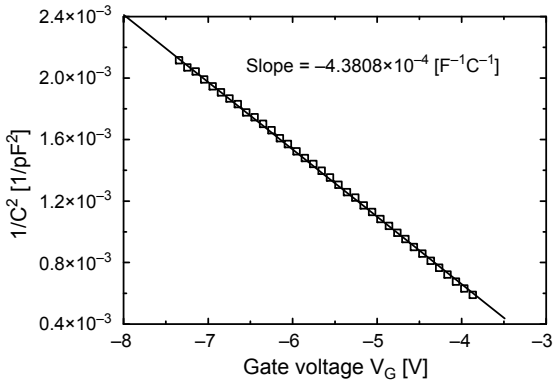

Fig. 2. The linear part of the $1/C^2 = f(V_G)$ plot measured on the Al–SiO_2–SiC(3C) structure.

This method does not require any other information about the investigated structure than the value for the gate area A. An example of such a characteristic is shown in Fig. 2.

The N_D value is used to calculate the Fermi potential ϕ_F using the formula [7]:

$$\phi_F = -\frac{kT}{q}\ln\left(\frac{N_D}{n_i}\right) \tag{5}$$

where: n_i – intrinsic concentration in the substrate [cm^{-3}].

To determine n_i, the following formula was used [1]:

$$n_i = \sqrt{N_C N_V}\,\exp\left(-\frac{qE_G}{2kT}\right) \tag{6}$$

where: E_G – energy bandgap [eV], N_C, N_V – effective density of states in the conduction and valence band, respectively, $N_C = 1.353\times10^{19}$ cm^{-3}, $N_V = 1.006\times10^{19}$ cm^{-3} [1].

3.2. Optical properties

To determine the barrier heights in a MOS structure using the Fowler method [8], the so-called RTA values of the structure have to be calculated as a function of the wavelength of the light used in photoelectric measurements. In the term RTA, R is the fraction of light power reflected from the structure, T is the fraction absorbed by the substrate and A is the fraction absorbed by the gate. In our calculations of these characteristics, using methods described in [6, 11], the optical indices (refractive index – n, extinction coefficient – k) were taken from literature [12]. It was noted that our spectroellipsometric measurements fully confirmed the values given in [12]).

An example of RTA = $f(\lambda)$ characteristics calculated for the Al–SiO_2–SiC(3C) structure with Al thickness t_{ME} = 25 nm and SiO_2 thickness t_{OX} = 59.84 nm is shown in Fig. 3.

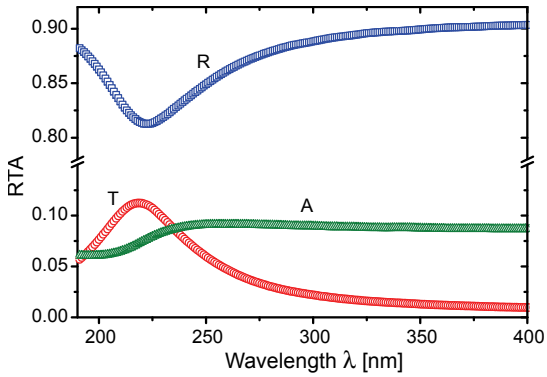

Fig. 3. RTA = $f(\lambda)$ characteristics calculated for Al–SiO_2–SiC(3C) structure (t_{ME} = 25 nm, t_{OX} = = 59.84 nm).

3.3. Photoelectric measurements

Energy barrier heights at the metal–dielectric (E_{BG}) and dielectric–semiconductor (E_{BS}) interfaces were determined using the photoelectric Fowler method [13, 14]. This method consists in transforming the measured photocurrent vs. wavelength characteristics at different gate biases (V_G) (negative V_G for E_{BG} determination, positive for E_{BS}) into the $Y^{1/p} = f(h\nu)$ dependences. Where Y is the photoemission yield, $h\nu$ is photon energy and p is the exponent which assumes values $p = 2$ for electron emission from metal gate and $p = 3$ for electron emission from semiconductor substrate. The $Y^{1/p} = f(h\nu)$ dependence is a straight line for each of the gate biases used. Extrapolation of these straight lines to the $Y^{1/p} = 0$ value determines the value of $h\nu(Y^{1/p} = 0)$, for each of the V_G values. Taking these $h\nu(Y^{1/p} = 0)$ values and plotting them versus $V_{OX}^{1/2}$, where V_{OX} is the voltage drop in the dielectric layer, one obtains a straight line again. Extrapolation of this straight line to the $V_{OX} = 0$ value gives the final barrier height $E_B = h\nu(Y^{1/p} = 0, V_{OX} = 0)$ value.

An example of the spectral characteristics obtained for the Al–SiO_2–SiC(3C) structure for positive V_G values is shown in Fig. 4**a**. Also, the calculated $h\nu(Y = 0) = f(V_{OX}^{1/2})$ dependence is shown (Fig. 4**b**).

Calculation of the photoemission yield Y, which is defined as the photocurrent normalized to the photon flux incident on the emitter, requires the knowledge of the RTA = $f(\lambda)$ characteristics discussed in Section 3.2.

The theory of internal photoemission (IPE) at low electric fields, applied to the dielectric of MOS structures developed in our laboratory [15], allows measurement of further parameters which are necessary to determine the complete band diagram of the structure under investigation. In particular, it allows determination of the gate voltage (V_{G0}) at which the voltage drop in the dielectric is equal to zero ($V_{OX} = 0$). It also allows accurate determination of the effective contact potential difference (ϕ_{MS}) between the gate and the substrate and of the semiconductor surface potential (ϕ_{S0}) as discussed below.

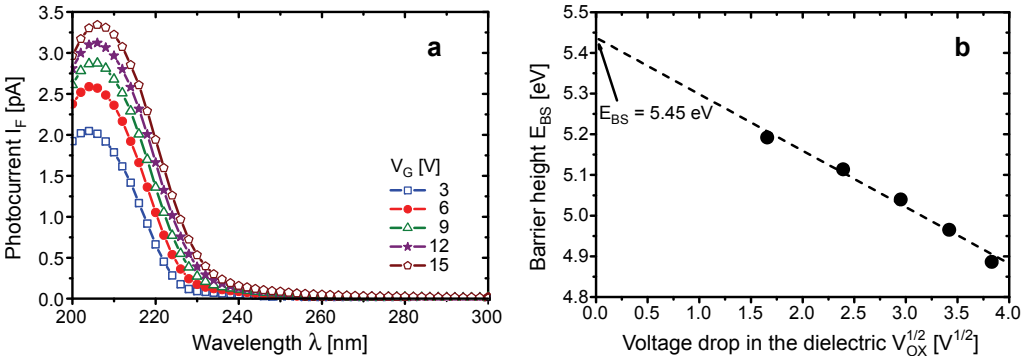

Fig. 4. Experimental spectral characteristics $I_F = f(\lambda)$ obtained for the Al–SiO_2–SiC(3C) structure for positive gate voltages V_G (**a**). The calculated $h\nu(Y = 0) = f(V_{OX}^{1/2})$ dependence (**b**).

These measurements are based on measuring photocurrent vs. gate voltage ($I_F = f(V_G)$) characteristics at different wavelengths, in the vicinity of the $I_F = 0$ point. Such characteristics intersect the $I_F = 0$ axis at different values of gate voltage (V_G^0) depending on the wavelength λ. As shown in [15] the $I_F = f(V_G)$ characteristic which is symmetrical with respect to the $I_F = 0$ point, intersects this axis at $V_G = V_{G0}$, which corresponds to the situation when the bands in the dielectric are flat ($V_{OX} = 0$). The wavelength resulting in the symmetrical $I_F = f(V_G)$ characteristic is $\lambda = \lambda_0$.

An example of $I_F = f(V_G)$ characteristics for different λ values in the vicinity of the $I_F = 0$ point is shown in Fig. 5.

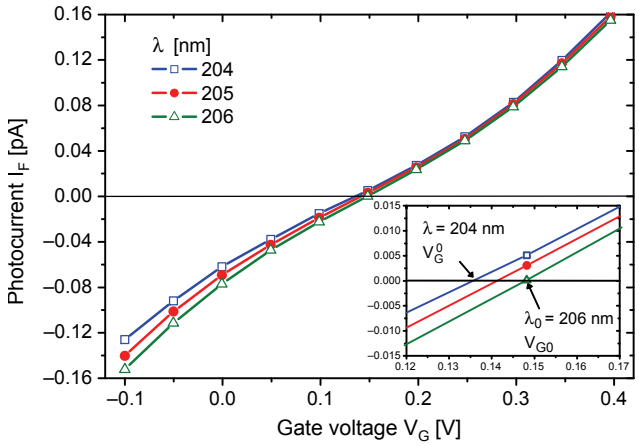

Fig. 5. Experimental $I_F = f(V_G)$ characteristics measured on the Al–SiO_2–SiC(3C) structure. Measurements were made at different wavelengths λ in order to determine the V_{G0} voltage.

Another parameter which plays a significant role in determining the band diagram of the MOS structure is the surface potential of the semiconductor (ϕ_{S0}) corresponding to the flat-band state in dielectric ($V_G = V_{G0}$). The method to determine ϕ_{S0} applied in this work is based on measurement of the $I_F = f(V_G)$ characteristics at different λ and on measurement of the capacitance under illumination $C^* = f(V_G)$ characteristic (shown in Fig. 1). The $C^* = f(V_G)$ characteristic should be measured for the wavelength λ_0 and for the same light power P for which V_{G0} value was obtained. Using the V_{G0} value and $C^* = f(V_G)$ characteristic, the capacitance $C^*(V_{G0})$ value can be determined which is further used in calculation of the surface semiconductor capacitance $C_S^*(V_{G0})$:

$$C_S^*(V_{G0}) = \frac{C_{OX} C^*(V_{G0})}{C_{OX} - C^*(V_{G0})} \tag{7}$$

where: $C^*(V_{G0})$ – the capacitance for the gate voltage $V_G = V_{G0}$.

The $C_S^*(V_{G0})$ parameter is related to the surface potential (ϕ_{S0}) as shown in Eq. (8). This formula is valid for *n*-type substrates and for V_{G0} values located in the accumulation range (as in our case):

$$C_S^*(V_{G0}) = \sqrt{\frac{q^2 \varepsilon_S \varepsilon_0 N_D}{2kT}} \frac{e^{u_{S0}} - 1}{\sqrt{e^{u_{S0}} - u_{S0} - 1}} \tag{8}$$

$$u_{S0} = \frac{q}{kT} \phi_{S0} \tag{9}$$

Numerical iteration of Eq. (8) for a set of u_{S0} values permits determination of the u_{S0} value for which Eq. (8) is fulfilled, and thereby through Eq. (9) the ϕ_{S0} value can be obtained.

4. Measurement results

The photoelectric measurements of barrier heights E_{BG} at the Al–SiO_2 interface, and E_{BS} at the SiC(3C)–SiO_2 were fully reproducible. The mean E_{BS} barrier height value of ≈ 5.45 eV is lower than E_{BS} values found in the literature [16]. This is due to the fact that photoelectrons that constitute the photocurrent are not only emitted from the SiC valence band, but also from a band of high density interface states at SiC–SiO_2 interface. This band resides in the lower part of the SiC bandgap and probably results from the presence of carbon clusters in the SiO_2 in the vicinity of the SiC–SiO_2 interface [17]. This conclusion has been supported by the measurements of the interface trap density D_{it} (not discussed in the text).

The general representations of the band diagrams for the Al–SiO_2–SiC(3C) are shown in Fig. 6, for the flat-band state in the dielectric (**a**) and for the flat-band state in the semiconductor (**b**). These diagrams are primarily based on our measurement results with some data taken from the literature.

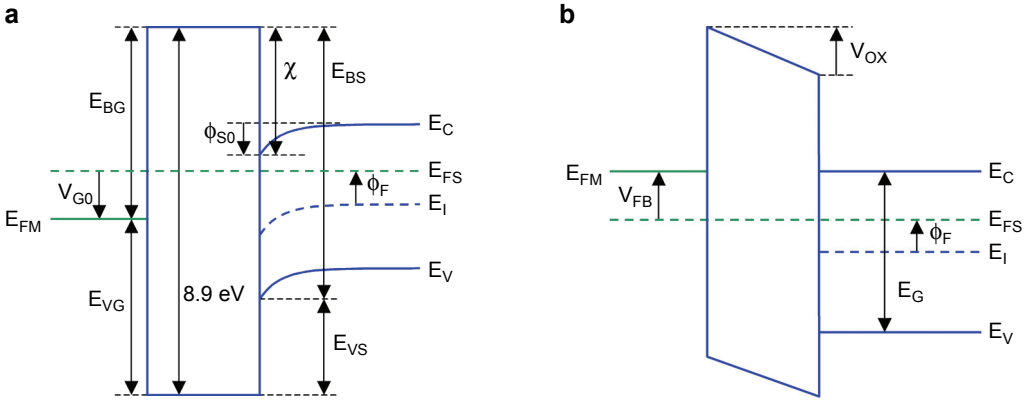

Fig. 6. The band diagram at the V_{G0} voltage (flat-band state in dielectric) – **a**, and at the V_{FB} voltage (flat-band in the semiconductor) – **b**, for the Al–SiO_2–SiC(3C) structures (not to scale).

The various potentials shown in Fig. 6 are calculated as follows:
– the electron affinity of the substrate at the interface χ [V]:

$$\chi = \frac{1}{q}(E_{\mathrm{BS}} - E_G) \tag{10}$$

– effective contact potential difference ϕ_{MS} [V]:

$$\phi_{\mathrm{MS}} = \frac{E_{\mathrm{BG}}}{q} - \left(\chi + \frac{E_G}{2q} + \phi_F\right) \tag{11}$$

– effective charge at the dielectric–semiconductor interface Q_{eff} [C/cm^2]:

$$Q_{\mathrm{eff}} = C_{\mathrm{OX}}\left(\phi_{\mathrm{MS}} - V_{\mathrm{FB}}\right) \tag{12}$$

– density of the N_{eff} [cm^{-2}]:

$$N_{\mathrm{eff}} = \frac{Q_{\mathrm{eff}}}{q} \tag{13}$$

At V_{G0}, the surface charge in the semiconductor (Q_S) is expressed as:

$$Q_S = -Q_{\mathrm{eff}} \quad (V_G = V_{G0}) \tag{14}$$

At V_{FB}, the voltage drop in the dielectric (V_{OX}) is given by:

$$V_{\mathrm{OX}} = -\frac{Q_{\mathrm{eff}}}{C_{\mathrm{OX}}} \quad (V_G = V_{\mathrm{FB}}) \tag{15}$$

The reproducibility of the barrier height measurements is very good, the standard deviation being $\sigma_{\mathrm{E}}(E_{\mathrm{BS}}) = 0.04$ eV and $\sigma_{\mathrm{E}}(E_{\mathrm{BG}}) = 0.02$ eV for many investigated structures. The absolute accuracy of the barrier height determination is estimated to be ±0.05 eV. The gate voltage value corresponding to the flat-band in the dielectric was found to be $V_{G0} = 0.148 \pm 0.020$ V, from which the effective contact potential difference ϕ_{MS} was calculated to be $\phi_{\mathrm{MS}} = 0.045 \pm 0.020$ V.

T a b l e. Barrier heights and other band diagram parameters of the Al–SiO_2–SiC(3C) structure.

E_{BG} [eV]	E_{BS} [eV]	E_{VG} [eV]	E_{VS} [eV]	χ [V]	ϕ_{F} [V]	ϕ_{MS} [V]
3.45	5.45	5.45	3.45	3.09	–0.96	0.045
Q_{eff} [C/cm^2]	N_{eff} [cm^{-2}]	ϕ_{S0} [V]	V_{G0} [V]	V_{FB} [V]	V_{OX} ($V_G = V_{\mathrm{FB}}$) [V]	
7.39×10^{-8}	4.61×10^{11}	0.103	0.148	–1.236	–1.281	

The barrier height measurement results have allowed determination of a complete set of parameters characterizing the band diagram of the investigated structure as described in the text and summarized in the Table.

5. Conclusions

The whole procedure to determine the band diagram of a MOS structure has been presented. Using electrical, photoelectric and optical methods, the numerous parameters of the MOS structure can be obtained. Among these parameters, the flat-band voltage in the semiconductor (V_{FB}) was determined from electrical measurements of $C = f(V_G)$ characteristics, and the flat-band voltage in the dielectric (V_{G0}) was determined using the high precision photoelectric method. The barrier heights E_{BG} and E_{BS} were determined using the photoelectric method taking into account the calculated optical properties (RTA characteristics) of the structures. Using the values of the above mentioned parameters, other properties of the structure under investigation were determined as shown in the Table and in Fig. 6.

References

[1] SHUR M., *SiC Parameters Handbook*, http://www.ioffe.ru/SVA/NSM/Semicond/SiC.

[2] PENSL G., BASSLER M., CIOBANU F., AFANAS'EV V.V., YANO H., KIMOTO T., MATSUNAMI H., *Traps at the SiC/SiO_2 interface*, MRS Proceedings **640**(3), 2000, p. H3.2.

[3] BAKOWSKI M., SCHÖNER A., ERICSSON P., STRÖMBERG H., NAGASAWA H., ABE M., *Development of 3C–SiC MOSFETs*, Journal of Telecommunications and Information Technology, No. 2, 2007, pp. 49–56.

[4] NAGASAWA H., ABE M., YAGI K., KAWAHARA T., HATTA N., *Fabrication of high performance 3C–SiC vertical MOSFETs by reducing planar defects*, [In] *Silicon Carbide: Volume 1: Growth, Defects, and Novel Applications*, [Eds.] Friedrichs P., Kimoto T., Pensl G., Wiley, New York, 2010.

[5] PORĘBSKI S., MACHALICA P., ZAJĄC J., BOROWICZ L., KUDLA A., PRZEWŁOCKI H.M., *Universal system for photoelectric characterisation of semiconductor structures*, IEE Proceedings Science, Measurement and Technology **150**(4), 2003, pp. 148–152.

[6] POWELL R.J., *Photoinjection into SiO_2: Use of optical interference to determine electron and hole contributions*, Journal of Applied Physics **40**(13), 1969, pp. 5093–5101.

[7] NICOLLIAN E.H., BREWS J.R., *MOS Physics and Technology*, J. Wiley and Sons, New York, 1982.

[8] HYNECEK J., *Graphical method for determining the flat band voltage for silicon on sapphire*, Solid-State Electronics **18**(2), 1975, pp. 119–120.

[9] YUN B.H., *Direct measurement of flat-band voltage in MOS by infrared excitation*, Applied Physics Letters **21**(5), 1972, pp. 194–195.

[10] JAKUBOWSKI A., KRAWCZYK S., *Photoelectric method of the MIS flat-band voltage determination*, Electron Technology **11**(1–2), 1978, pp. 23–35.

[11] HEAVENS O.S., *Optical Properties of Thin Solid Films*, Academic Press, New York, 1955.

[12] PALIK E.D. [Ed.], *Handbook of Optical Constants of Solids*, Academic Press Handbook Series, Orlando, 1985.

[13] AFANAS'EV V.V., *Internal Photoemission Spectroscopy: Principles and Applications*, Elsevier, 2008.

[14] FOWLER R.H., *The analysis of photoelectric sensitivity curves for clean metals at various temperatures*, Physical Review **38**(1), 1931, pp. 45–56.
[15] PRZEWŁOCKI H.M., *Theory and applications of internal photoemission in the MOS system at low electric fields*, Solid-State Electronics **45**(8), 2001, pp. 1241–1250.
[16] AFANAS'EV V.V., BASSLER M., PENSL G., SCHULZ M.J., STEIN VON KAMIENSKI E., *Band offsets and electronic structure of SiC/SiO_2 interfaces*, Journal of Applied Physics **79**(6), 1996, pp. 3108–3114.
[17] AFANAS'EV V.V., BASSLER M., PENSL G., SCHULZ M., *Intrinsic SiC/SiO_2 interface states*, Physica Status Solidi (a) **162**(1), 1997, pp. 321–337.

Received September 25, 2010